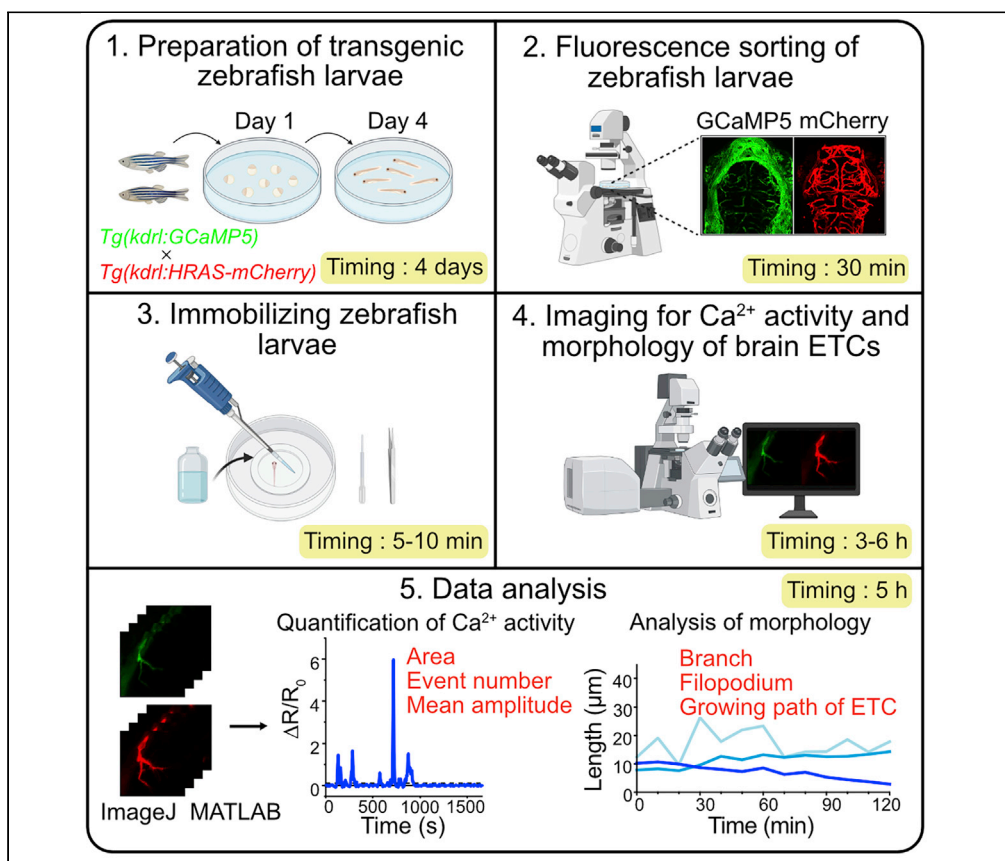


Protocol

A protocol for simultaneous Ca^{2+} and morphology imaging of brain endothelial tip cells in larval zebrafish



Endothelial tip cells (ETCs) located at growing blood vessels display high morphological dynamics and associated intracellular Ca^{2+} activities with different spatiotemporal patterns during migration. Examining the Ca^{2+} activity and morphological dynamics of ETCs will provide an insight for understanding the mechanism of vascular development in organs, including the brain. Here, we describe a method for simultaneous monitoring and relevant analysis of the Ca^{2+} activity and morphology of growing brain ETCs in larval zebrafish.

Ting-ting Liu, Han Hou, Jiu-lin Du

liutt2020@gmail.com (T.-t.L.)
forestdu@ion.ac.cn (J.-l.D.)

HIGHLIGHTS

Image Ca^{2+} activity of brain endothelial tip cells (ETCs) in larval zebrafish

Image the morphology of ETCs

Quantify the spatiotemporal pattern of Ca^{2+} activities in ETCs

Analyze the morphology of ETCs to trace the growing state

Liu et al., STAR Protocols 2, 100388
March 19, 2021 © 2021 The Author(s).
<https://doi.org/10.1016/j.xpro.2021.100388>



Protocol

A protocol for simultaneous Ca^{2+} and morphology imaging of brain endothelial tip cells in larval zebrafishTing-ting Liu,^{1,2,4,*} Han Hou,¹ and Jiu-lin Du^{1,2,3,5,*}

¹Institute of Neuroscience, State Key Laboratory of Neuroscience, Center for Excellence in Brain Science and Intelligence Technology, Shanghai Research Center for Brain Science and Brain-Inspired Intelligence, Chinese Academy of Sciences, 320 Yue-Yang Road, Shanghai 200031, China

²University of Chinese Academy of Sciences, 19A Yu-Quan Road, Beijing 100049, China

³School of Life Science and Technology, ShanghaiTech University, 319 Yue-Yang Road, Shanghai 200031, China

⁴Technical contact

⁵Lead contact

*Correspondence: liutt2020@gmail.com (T.-t.L.), forestdu@ion.ac.cn (J.-l.D.)
<https://doi.org/10.1016/j.xpro.2021.100388>

SUMMARY

Endothelial tip cells (ETCs) located at growing blood vessels display high morphological dynamics and associated intracellular Ca^{2+} activities with different spatiotemporal patterns during migration. Examining the Ca^{2+} activity and morphological dynamics of ETCs will provide an insight for understanding the mechanism of vascular development in organs, including the brain. Here, we describe a method for simultaneous monitoring and relevant analysis of the Ca^{2+} activity and morphology of growing brain ETCs in larval zebrafish. For complete details on the use and execution of this protocol, please refer to Liu et al. (2020).

BEFORE YOU BEGIN

The expansion of the brain vasculature in zebrafish begins at 2 days post-fertilization (dpf), and becomes robust at 3 dpf, remarkable by numerous growing vessels tipped with endothelial tip cells (ETCs) budding from the choroidal vascular plexus (CVP) located peripherally in the midbrain and migrating into the midbrain. Thus, ETCs budding from the CVP of 3-dpf zebrafish larvae are selected for imaging.

Production and maintenance of transgenic zebrafish larvae

⌚ Timing: 4 days

Double transgenic zebrafish *Tg(kdrl:GCaMP5,kdrl:HRAS-mCherry)* larvae are used for imaging, in which the GCaMP5 (a genetically encoded Ca^{2+} indicator) and mCherry (a cell membrane-bound red fluorescent protein) are specifically expressed in endothelial cells (ECs) including ETCs, to visualize Ca^{2+} activity and morphology of ETCs, respectively (Figure 1). The parental transgenic zebrafish *Tg(kdrl:GCaMP5)* line was generated by our lab as described in Liu et al. (2020), and the *Tg(kdrl:HRAS-mCherry)* line was a gift from Dr. Didier Stainier's lab (Chi et al., 2008).

1. Day 0. Mate adult fishlines of *Tg(kdrl:GCaMP5)* and *Tg(kdrl:HRAS-mCherry)* in a mating tank (Outside : 22.5 cm * 11.5 cm * 11.5 cm; Inner: 22.0 cm * 11.0 cm * 8.5 cm) with 2 pairs of male/female fish.



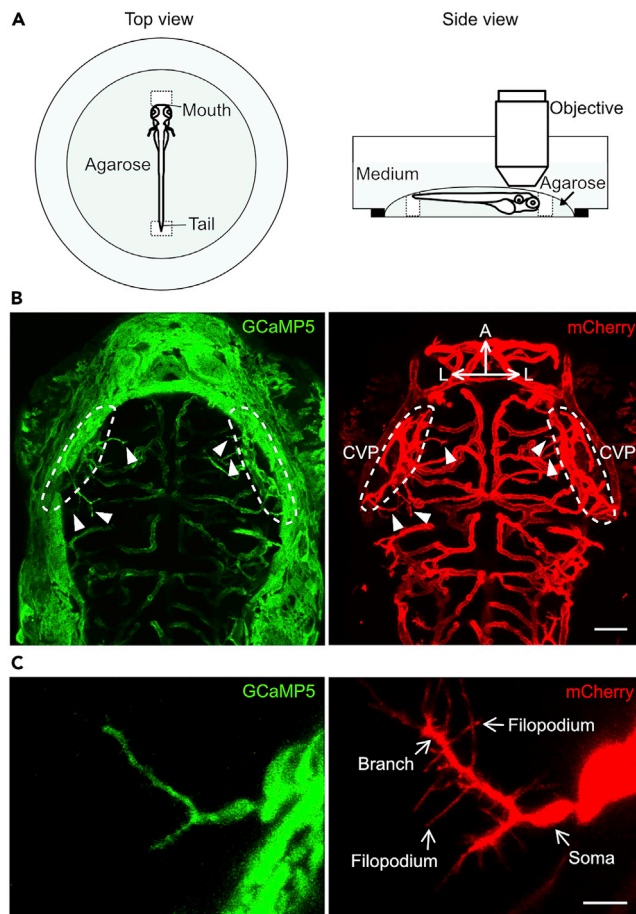


Figure 1. Schematic and example images showing confocal imaging of brain ETCs in larval zebrafish

(A) Schematic showing the setup for confocal imaging of brain ETCs in a immobilized zebrafish larva. Left, top view of the imaged zebrafish larva immobilized in the agarose of a glass coverslip-filled well of the plastic dish. Right, side view of the imaged zebrafish larva under the objective of the confocal microscope. White regions outlined with black dashed lines indicate free space with agarose removed around the mouth and tail of the larva. Green and light green colors indicate agarose and medium, respectively.

(B) Representative Z axis projected images showing the brain vasculature of a transgenic zebrafish *Tg(kdrl:GCaMP5,kdrl:HRAS-mCherry)* larva at 3 days post-fertilization (dpf). Green, GCaMP5 signal; red, mCherry signal. CVP is outlined by white dashed lines, and ETCs are indicated by white arrow heads. Scale bar, 50 μ m.

(C) Example images showing the expression of GCaMP5 and mCherry in brain ETCs. Scale bar, 10 μ m.

2. Day 1 (0 dpf). Collect fertilized eggs produced and maintain them under a 14 h/10 h light/dark cycle in Hank's solution (Westerfield, 2000). 6 h later, remove dead eggs and refresh the incubation medium.
3. Day 2 (1 dpf). Add 1-phenyl-2-thiourea (PTU) to the Hank's solution with a final concentration of 0.003% (w/v) to prevent pigment formation.
4. Day 3–4 (2–3 dpf). Maintain the embryos until 3 dpf for imaging experiment.
5. Day 4 (3 dpf).
 - a. Remove the PTU-contained medium, and wash embryos for 10 times with a clean medium, then collect them in a dish.
 - b. Pick up zebrafish larvae carrying the expression of both GCaMP5 and mCherry by using a soft plastic straw under a mercury lamp microscope.

Note: The motility of zebrafish larvae at 3 dpf is usually low, making it possible to place free-moving larvae under the microscope for sorting. For zebrafish larvae exhibiting high

locomotion activity, the larva should be immobilized with low-melting point agarose beforehand. In addition, when picking up larvae carrying the expression of GCaMP5 and mCherry under the fluorescence microscope, the wide expression of GCaMP5 in endothelial cells of the brain vasculature should be confirmed under both low (10×) and high (40×) magnification fields of view, as the GCaMP5 fluorescence is relatively weak.

△ **CRITICAL:** Do not use Tricaine methanesulfonate (MS222) for anesthesia in this experiment. The anesthetic effect of MS222 acts through inhibiting the entrance of sodium ions into the cell, thus inhibiting action potentials in neurons (Carter et al., 2011). Previous evidence has shown the expression of sodium channels in ECs and these channels are required for angiogenesis (Andrikopoulos et al., 2011; Gordienko and Tsukahara, 1994). Furthermore, we found that treatment of MS222 largely affects the morphology of ETCs, with obvious retraction of ETC filopodia and branches.

KEY RESOURCES TABLE

REAGENT or RESOURCES	SOURCE	IDENTIFIER
Chemicals, peptides, and recombinant proteins		
1-Phenyl-2-thiourea (PTU)	Sigma-Aldrich	Cat #: P7629
Na ₂ HPO ₄	Sigma-Aldrich	Cat #: S0876
KH ₂ PO ₄	Sigma-Aldrich	Cat #: P5379
MgSO ₄ ·7H ₂ O	Sigma-Aldrich	Cat #: 63138
NaHCO ₃	Sigma-Aldrich	Cat #: S5761
MgCl ₂ ·6H ₂ O	Sigma-Aldrich	Cat #: M9272
HEPES	Sigma-Aldrich	Cat #: H4034
D-Glucose	Sigma-Aldrich	Cat #: G8270
Low-melting point agarose	Thermo Fisher Scientific	Cat #: 16520100
Experimental models: organisms/strains		
Zebrafish (3 months to 1 year old, male/female): <i>Tg(kdrl:HRAS-mCherry)</i>	Chi et al., 2008	ZFIN ID: ZDB-ALT-081212-4
Zebrafish (3 months to 1 year old, male/female): <i>Tg(kdrl:GCaMP5)</i>	Liu et al., 2020	N/A
Software and algorithms		
NIS-Elements Viewer Version 4.20	Nikon, Japan	N/A
ImageJ	National Institute of Health, USA	https://imagej.nih.gov/ij/index.html
Self-written MATLAB program to discriminate Ca ²⁺ transients	Liu et al., 2020	This paper
MATLAB	MathWorks	R2017b
Other		
Self-designed 35-mm plastic dish with a glass coverslip-filled well	Thermo Fisher Scientific; Sigma-Aldrich	Cat #: 150318; C9802
Nikon FN1 confocal microscope	Nikon, Japan	Eclipse FN1
Microscope heat controller	Nanjing Kel, China	KEL-2000

MATERIALS AND EQUIPMENT

Preparation of Hank's solution

To make the Hank's solution, prepare all five stock solutions mentioned below, and store them at 4°C for up to several months. Make a premix by combining the stock solutions in the following order and quantities: 100 mL Stock #1, 10 mL Stock #2, 10 mL Stock #3, 10 mL Stock #4, and 860 mL H₂O. Store the premix at 4°C for up to several weeks. Just before use, add 10 mL Stock #5 to the premix, and adjust the pH to 7.2 with NaOH.

Stocks	Reagents	Amount (g) for 1 L	Final concentration in Hank's solution (mM)
Stock #1	NaCl	81.8	140
	KCl	4.0	5.4
Stock #2	Na ₂ HPO ₄	3.58	0.25
	KH ₂ PO ₄	6.0	0.44
Stock #3	CaCl ₂	14.4	1.3
Stock #4	MgSO ₄ ·7H ₂ O	24.6	1
Stock #5	NaHCO ₃	35	4.2
H ₂ O		To a final volume of 1 L for each stock	N/A

Preparation of external solution (ES)

Reagents	Amount (g) for 1 L	Final concentration (mM)
NaCl	7.83	134
KCl	0.22	2.9
CaCl ₂ ·2H ₂ O	0.31	2.1
MgCl ₂ ·6H ₂ O	0.24	1.2
HEPES	2.38	10
D-Glucose	1.80	10
ddH ₂ O	To a final volume of 1 L	N/A

Adjust the pH to 7.8 with 10 M NaOH, Osm 290. Keep at 4°C for up to 1 week.

Preparation of 1.2% low-melting point agarose

To prepare the 1.2% low-melting point agarose, dissolve the agarose via heating, then incubate the

Reagents	Amount	Final concentration (%)
Low-melting point agarose	0.06 g	1.2
ES	5 mL	N/A

agarose solution at 37°C for usage.

STEP-BY-STEP METHOD DETAILS

Immobilizing zebrafish larvae

⌚ Timing: 5–10 min

1. Immobilize the larvae with 1.2% low-melting point agarose in a self-designed 35-mm plastic dish with a glass coverslip-filled well. Then incubate the larvae with ES, and remove the agarose around the larva's mouth and tail with a fine-tipped forceps to leave space for larva growth (Figure 1A).

Note: For making the dish, we drilled a hole in the lid of a commercial petri dish, then glued a circular or square glass coverslip to fill the hole.

⚠ CRITICAL: Removing agarose to leave free space for the mouth and tail of the larva is important for relieving mechanical restriction on the growing body length of the larva. Do not skip this step.

Imaging for Ca²⁺ activity and morphology of ETCs

⌚ Timing: 3–6 h

2. Prepare the Nikon FN1 confocal microscope equipped with a 25 × (NA 1.1) or 40 × (NA 0.8) water-immersion objective and a heating system with the incubation temperature of 28°C.
3. Open the NIS-Elements Viewer imaging software, and set parameters for the time-lapse imaging. Use lasers of 488 nm and 561 nm to excite GCaMP5 (for Ca²⁺ activity) and mCherry (for morphology) of ETCs, respectively.
4. Identify ETCs for imaging. Place the larva-contained dish under the objective lens of the microscope, find the field of the brain using bright field. Perform a XYZ image of the brain vascular network with GCaMP5 and mCherry at the Z-axis resolution of 4 μm to identify CVP located peripherally in the midbrain. Then identify the ETCs budding from the CVP and extending into the midbrain with several sub-cellular branches and numerous filopodia in the image (Figures 1B and 1C). Finally, move the confocal plane in Z-axis to the identified ETC for the following imaging process.
5. Perform time-lapse imaging for the selected ETC for 3 – 6 h (Figure 1). The spatial resolution for images is 0.2–0.4 μm per pixel, the Z-axis resolution is 4 μm, and the interval for Z-projected time-lapse images is ~ 6 s. During the imaging process, include separated imaging cassettes with time length of 30 min. At the beginning of each imaging cassette, refresh ES solution in the dish through removing old solution and supplementing fresh solution to maintain the larva in a good condition, and reset the bottom-/up- imaging boundary in Z-axis to cover the complete morphology of the ETC.

⚠ **CRITICAL:** The interval for Z-projected time-lapse images is an important parameter in this imaging experiment, and too long imaging interval (e.g., larger than half time of the duration of Ca²⁺ transients) should be avoided, as it could miss Ca²⁺ transients with relative small duration. Based on our imaging data, the average duration of Ca²⁺ transients in ETCs is 40.4 ± 2.3 s. We used the interval of ~ 6 s in our experiments, which is just enough for capturing Ca²⁺ transients in ETCs. Consistently, Yokota *et al* used 5 s as the interval for monitoring Ca²⁺ oscillations of ECs in larval zebrafish (Yokota *et al.*, 2015). Some ETCs engage the widely distributed morphology in the Z-axis, and more optical sections in Z-axis are required to cover the complete morphology of the ETC, and a longer imaging interval is needed as a result. For this condition, these ETCs should be avoided for imaging.

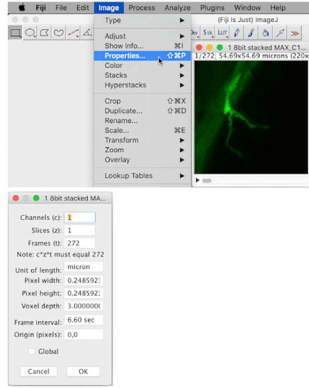
Note: To avoid large fluctuation of the imaging region in Z-axis during time-lapse imaging, it is important to include separated imaging cassettes according to the imaging time length with reset of bottom-/up- imaging boundary in Z-axis for each imaging cassette.

Analysis of Ca²⁺ imaging data

⌚ Timing: 3 h

6. Ratiometric analysis of Ca²⁺ activities of ETCs in *Tg(kdrl:GCaMP5,kdrl:HRAS-mCherry)* larvae using ImageJ (NIH) (Figure 2).
 - a. Adjust the properties of the time-lapse images, including unit of length (micron), pixel width/height, and voxel depth (Figure 2A). Then export the image series into a Z-axis projected “tif” image file with the type of 8 bit.
 - b. To correct movement of images within the same time-lapse image series, all images should be aligned with the reference image. Choose one image with obvious Ca²⁺ activity and relatively least movement at X-Y plane as the reference image in the GCaMP5 image series (Figure 2B), then align the analyzed images series with the reference image along X-Y plane using the Translation Transformation plugin (Figure 2C).

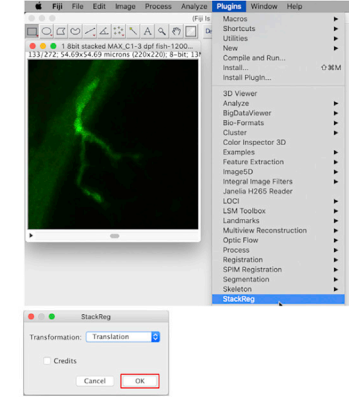
A Adjust properties of the 8-bit series



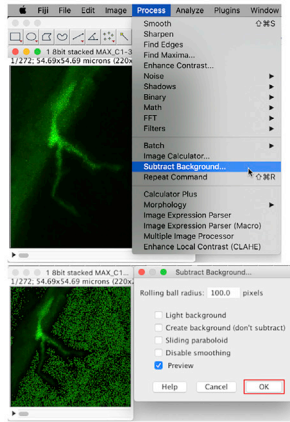
B Selection of the reference image



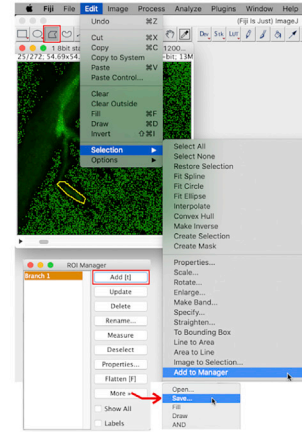
C Align series with the reference image



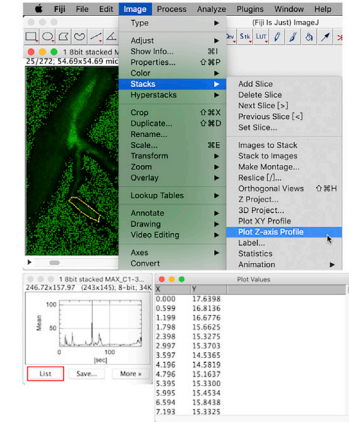
D Background subtraction



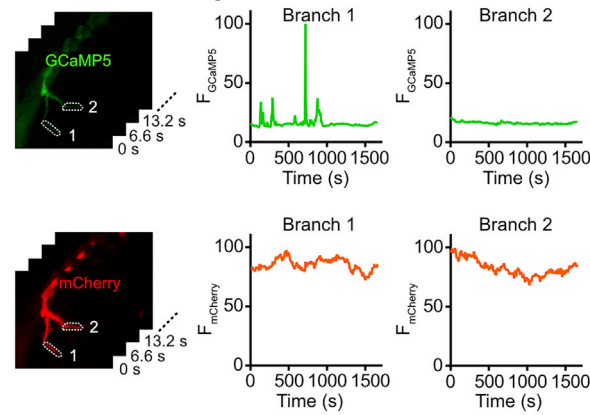
E Region of interests (ROI) selection



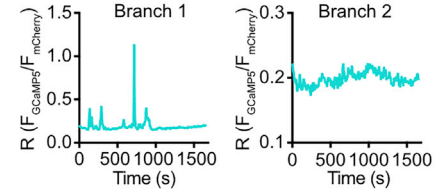
F Gray-scale value extraction



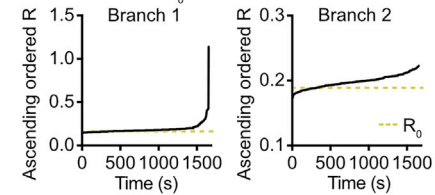
G Plot of F values in image series



H Generation of R values



I Calculation of R₀



J Calculation of $\Delta R/R_0$

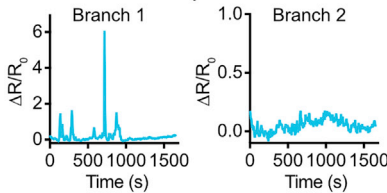


Figure 2. Pipeline and example case for ratiometric analysis of Ca²⁺ activities in ETCs

This procedure consists of adjust properties of the 8-bit series (A), selection of the reference image (B), align series with the reference image (C), background subtraction (D), ROI selection (E), gray-scale value extraction (F), plot F values in image series (G), generation of R values (H), calculation of R₀ (I), and calculation of $\Delta R/R_0$ (J). For each step, example operation with ImageJ (A–F) or plotted Ca²⁺ trace (G–J) is displayed.

Note: Images with the same sequential number should be used for the reference images in the GCaMP5 and mCherry image series in the same time-lapse imaging data.

- c. Subtract the background of the analyzed image series and draw the region of interest (ROI) manually to outline the morphology of ETC branches, soma, or other sub-cellular structures, then quantify the gray-scale value of each ROI as F (Figures 2D–2G).
- d. Generate R values with the ratio of $F_{\text{GCaMP5}}/F_{\text{mCherry}}$ (Figure 2H).
- e. Calculation of R₀. Plot R values with the ascending order, the averaged value of the first 100 frames is defined as R₀ (Figure 2I).

Note: The number of frames used for calculating the average value in generating R₀ depends on the length of the analyzed time-lapse image series. It is important that R values within the Ca²⁺ transients of ETCs should be avoided for R₀ calculation. Usually, 100 frames are enough for calculating R₀ in an image series containing about 300 frames.

- f. Calculate $\Delta R/R_0$ with the equation of $(R - R_0)/R_0$ (Figure 2J).
7. Calculate the peak magnitude, duration, and number of Ca²⁺ transients with a self-written MATLAB program (Figure 3).
- a. To exclude the effect of possible fluctuation of the baseline of Ca²⁺ activities during *in vivo* long-term imaging, an adaptive and iterative algorithm to detect Ca²⁺ transients was designed, as briefly introduced as follows,
 - i. Iterate the two steps until convergence: first, calculate a smoothed baseline from a baseline set; second, update the baseline set by removing potential Ca²⁺ transients from the smoothed baseline. Values larger than 3 times of standard deviation (STD) are considered as data points in a potential Ca²⁺ transient.

Note: For very sharp fluctuation in the baseline of Ca²⁺ traces, errors may happen in predicting the data in the baseline as in the Ca²⁺ transient. To solve this problem, data before and after the fluctuation point should be separately analyzed.

- ii. Upon convergence, define actual Ca²⁺ transients as the potential Ca²⁺ transients with duration longer than 15 s.
- Note:** Our previous data (Liu et al., 2020) and other literature (Yokota et al., 2015) showed that the duration of spontaneous Ca²⁺ transients of ETCs is usually larger than 15 s in zebrafish larvae. Therefore, we define the duration of 15 s as the criteria for defining actual Ca²⁺ transients. This value could be adapted with some special properties of Ca²⁺ transients in imaged ETCs during analysis.
- iii. Generate the final-baseline-subtracted Ca²⁺ trace and quantify Ca²⁺ transient properties based on this trace.
- b. Copy the dataset containing time and $\Delta R/R_0$ values into an Microsoft Excel data file with the column title of "Time (s)" and "Delta R/R₀," respectively (see example data file, Data S1).
 - c. Run the MATLAB script (Data S2) and select the data file(s) when prompted. The script will show the iteration process, the final baseline-subtracted Ca²⁺ trace, and the quantification data including the area, mean amplitude, and number of Ca²⁺ transients.

△ CRITICAL: The baseline and Ca²⁺ transients of the baseline-subtracted Ca²⁺ trace should be further confirmed with the Ca²⁺ trace before baseline subtraction through graphs plotted from this program, to ensure proper background removal and Ca²⁺ transient detection. The three parameters in the script can be adjusted if necessary (the baseline

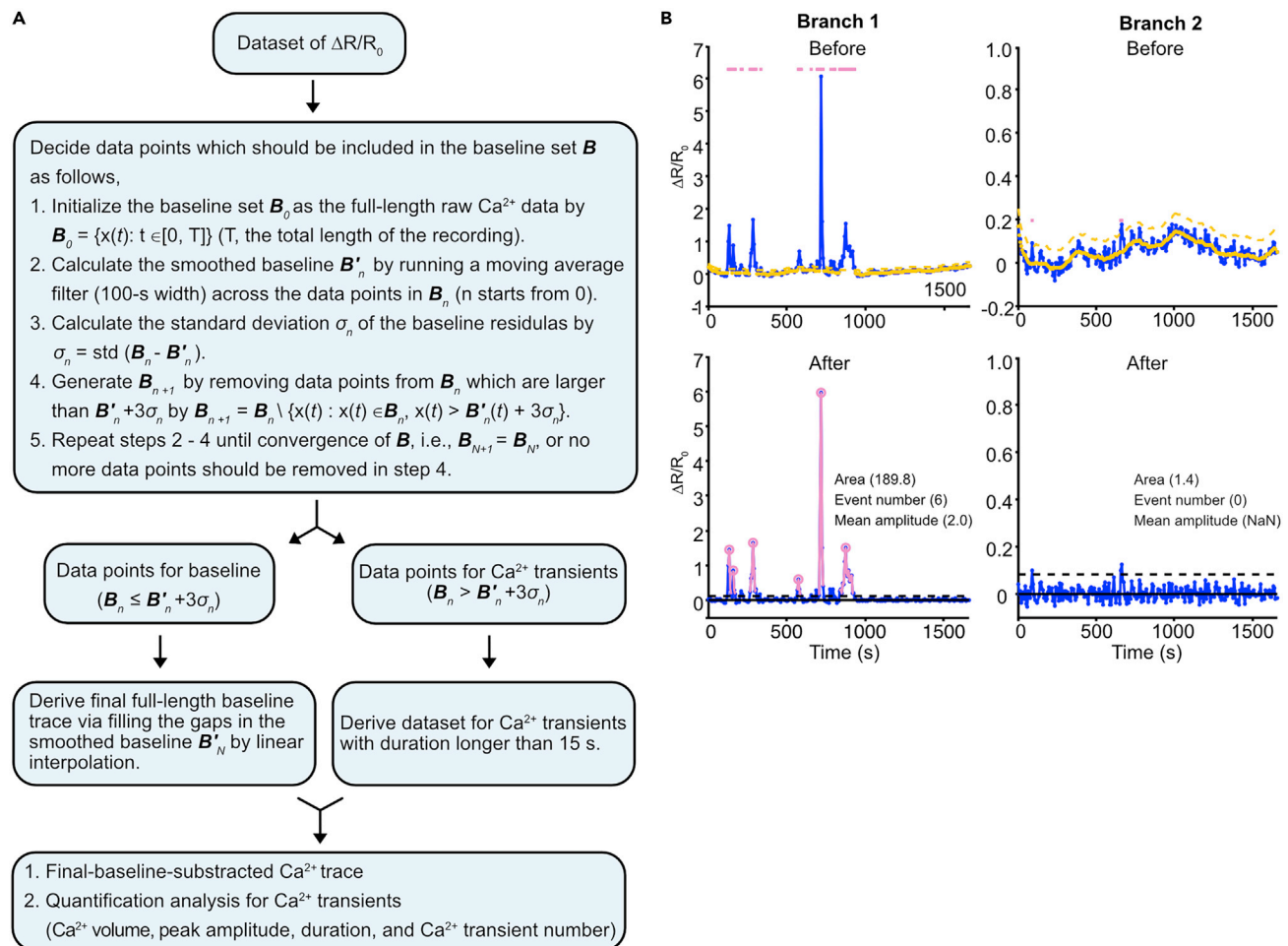


Figure 3. Pipeline and example case showing quantification of Ca^{2+} transients in ETCs

(A) Pipeline showing the algorithm in the self-written MATLAB program for quantifying Ca^{2+} transients in ETCs based on the dataset of $\Delta R/R_0$. (B) Example showing Ca^{2+} traces before (top panels) and after (bottom panels) baseline subtraction and quantification for Ca^{2+} transients. The same Ca^{2+} traces were used as shown in Figure 2. In the top panels, the yellow thick and dashed lines indicate the smoothed baseline and the threshold for potential Ca^{2+} transients (marked by pink dots on the top) upon convergence, respectively. In the bottom panels, the baseline (black thick line) has been removed from the raw data, and the actual Ca^{2+} transients are annotated (pink lines with circles indicating the peaks). Area, the total area of Ca^{2+} transients in the calculated trace; event number, the number of Ca^{2+} transients; mean amplitude, the averaged peak value of Ca^{2+} transients.

smooth window, the number of standard deviation that defines the threshold of potential transients, and the minimal duration that defines the actual Ca^{2+} transients). In addition, for errors caused by identified artificial Ca^{2+} transients because of large movements of images instead of actual Ca^{2+} activity of ETCs, it should be corrected manually in the process of quantification for Ca^{2+} transients, through removing the calculation for these Ca^{2+} transients including the area, amplitude, and number of Ca^{2+} transients.

Δ **CRITICAL:** For the kinetics of Ca^{2+} transients in ETCs, we collected our imaging data and performed analysis on 79 Ca^{2+} transients of branches from 22 ETCs, and 32 Ca^{2+} transients of somata from 11 ETCs. It shows that heterogeneity exist among these Ca^{2+} transients, with the exhibition of both single-peaked events and accumulated-fired multiple-peaked events (Figure 4A). To further analyze the timing property of Ca^{2+} transients in ETCs, including the duration, rise time, and decay time of Ca^{2+} transients in branches or somata of ETCs, we generated a MATLAB script for Ca^{2+} transients fitting via modeling

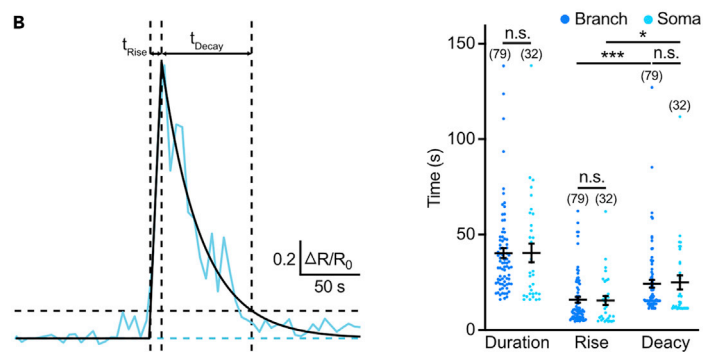
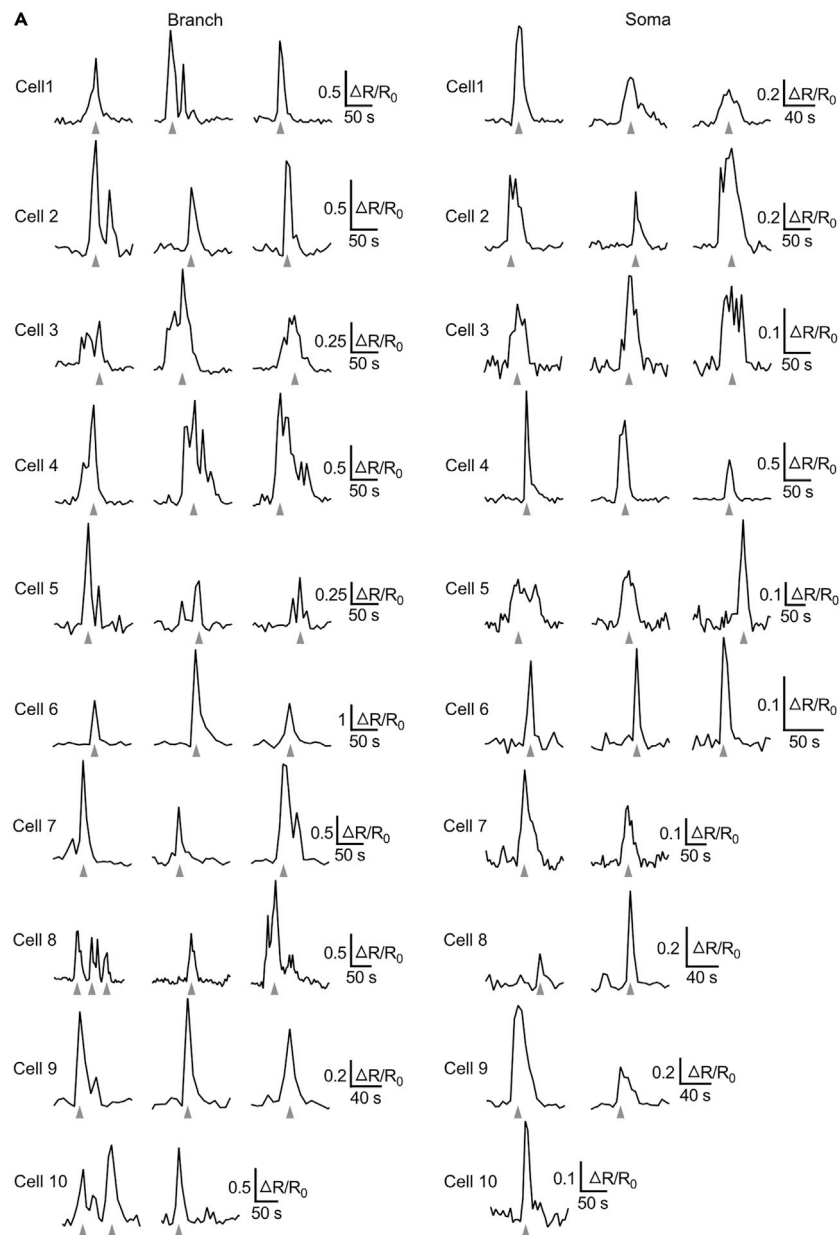


Figure 4. Example traces and kinetic analysis of high-resolution Ca^{2+} transients in the branches and somata of ETCs
(A) Example traces showing Ca^{2+} transients with high-resolution in the branches (left) and somata (right) of ETCs. For each group, Ca^{2+} transients from 10 cells were plotted.
(B) Schematic showing method for analysis and summary of the duration, rise time, and decay time of Ca^{2+} transients in ETC branches and somata. In the left Ca^{2+} traces, the blue and black trace represent Ca^{2+} transient before and after fitting, respectively. The blue and black weak lines indicate the baseline and threshold with 90% decay of the peak of the fitted Ca^{2+} transient, respectively. t_{Rise} , rise time of the Ca^{2+} transient; t_{Decay} , decay time of the Ca^{2+} transient. The numbers in the brackets indicate the numbers of Ca^{2+} transients in ETC branches or somata. n.s., no significance; * $p < 0.05$, *** $p < 0.001$ (two-tailed Mann-Whitney test). Mean \pm SEM.

the rise and decay phases of Ca^{2+} transients as linear and exponential, respectively. Through defining the threshold as 90% decay of the peak of the fitted Ca^{2+} transient, the duration (with $\Delta R/R_0$ above the threshold), rise time (time between the threshold and the peak in the rise phase), and decay time (time between the threshold and the peak in the decay phase) were then calculated (Figure 4B). For the duration of Ca^{2+} transients, it shows no significant difference between the branches and somata of ETCs (branch versus soma, 40.3 ± 2.6 s versus 40.5 ± 4.9 s, $p = 0.6$, two-tailed Mann-Whitney test). Furthermore, there is no significant difference for the rise and decay time between the branches and somata of ETCs, respectively (rise time, branch versus soma, 16.0 ± 1.5 s versus 15.5 ± 2.3 s, $p = 0.6$; decay time, branch versus soma, 24.3 ± 2.0 s versus 25.0 ± 3.6 s, $p = 0.2$, two-tailed Mann-Whitney test). Meanwhile, the rise time is significantly shorter than the decay time of Ca^{2+} transients in both branches and somata of ETCs (branch, rise versus decay, 16.0 ± 1.5 s versus 24.3 ± 2.0 s, $p < 0.0001$; soma, rise versus decay, 15.5 ± 2.3 s versus 25.0 ± 3.6 s, $p = 0.01$; two-tailed Mann-Whitney test) (Figure 4B).

Analysis of morphology of ETCs

⌚ Timing: 2 h

8. Calculate the length of ETC branches, ETC filopodia, or ETC growing path using ImageJ (Figure 5).
 - a. Adjust the property and contrast of the mCherry time-lapse image series and export it into a Z-projected "tif" image file with the type of 8-bit.
 - b. Duplicate one single image from the series for tracing at the analyzed time point.
 - c. Open the Simple Neurite Tracer plugin, and define the start (root) and end (tip) positions of the calculated ETC branch, ETC filopodium, or growing ETC.

Note: For ETC branch, the start (root) position is the branching site between the traced branch segment and its parental branch segment, and the end (tip) position locates in the free terminal of this traced branch. While for ETC filopodium, these two positions are located in the branching site between the traced filopodium segment and its parental branch/filopodium segment, and its free terminal, respectively. For the growing path of ETC, each branch segments of the ETC should be traced, starting from the root position located in the budding site between the traced ETC and the parental vessel in CVP, and ending in positions of free terminal sites of each terminal branch. Finally, the sum of calculated length for each traced path segments is the length of growing path of the analyzed ETC.

- d. Choose "Keep the new path segment" and "Finish path," then the path is traced and calculated for the length.
- e. Save the trace and dataset. Using this method, the retraction or extension of ETC branches and filopodia, or growing path of ETCs can be quantitatively defined or calculated.

Note: The above tracing method is suitable for the morphological analysis of X-Y plane-distributed ETC branch, filopodium, or growing path. Alternatively, for the analysis of ETC

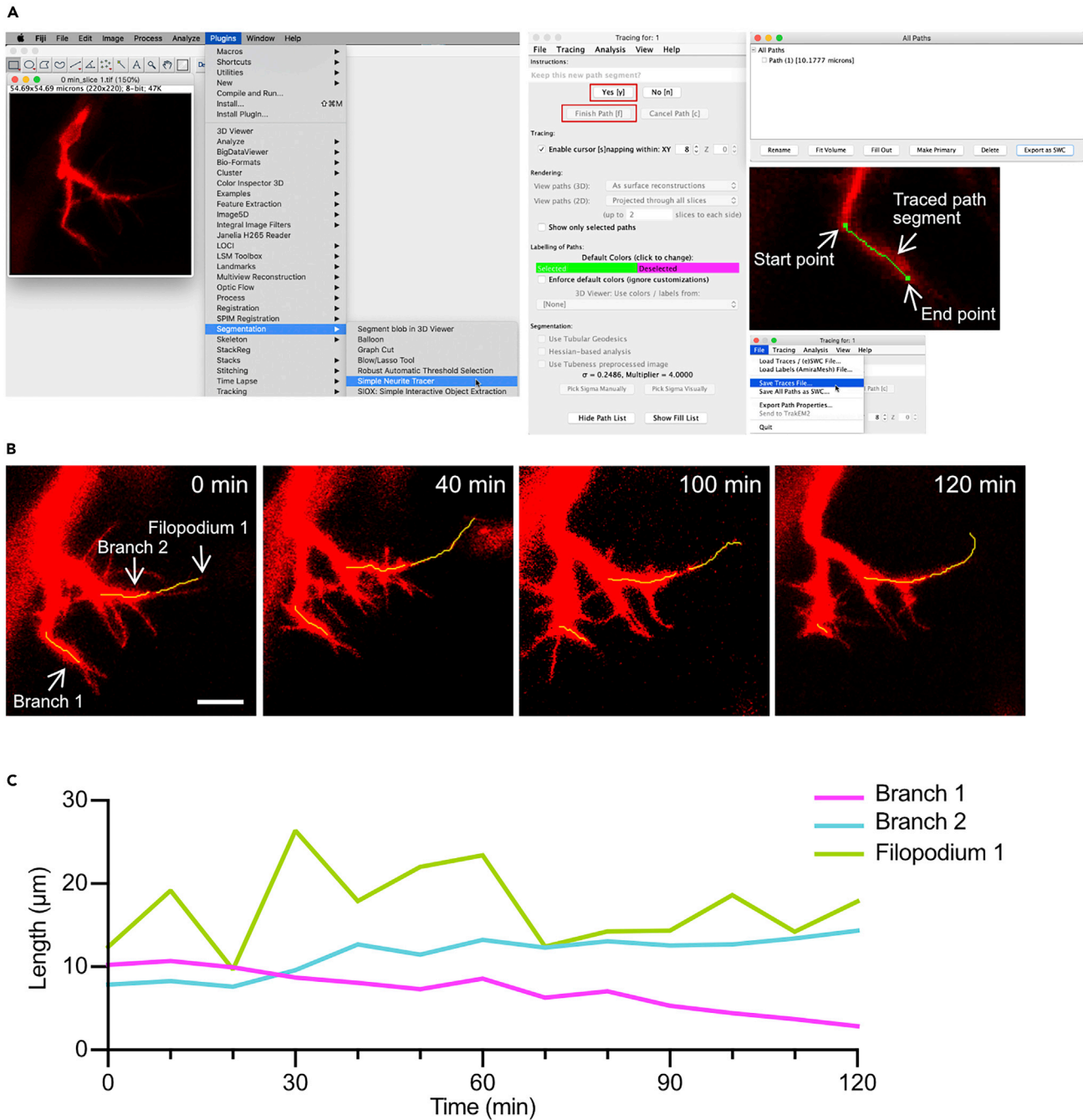


Figure 5. Morphological analysis on the length of ETC branches and filopodia

(A) Pipeline showing the tracing method using ImageJ.

(B) Example showing analysis on tracing the morphology of ETC branches and filopodia in time-lapse images. Two ETC branches and one filopodium from the same ETC analyzed in Figures 2 and 3 were traced. The yellow line indicates the traced path of the branches or filopodia of ETCs. Scale bar, 10 μm .

(C) Time course of the calculated length of ETC branches and filopodia. Branch 1 (magenta) and branch 2 (blue) display retracting and extending dynamics, respectively. Meanwhile, filopodium 1 (green) shows frequent retracting and extending dynamics along with the imaging period of 120 min.

morphologies with relatively wide distribution in the Z plane, the 3D tracing method should be adaptively used. For this condition, the analyzed image should be Z-axis non-projected, and the 3D Simple Neurite Tracer plugin should be used for the tracing.

- Define morphological dynamics of ETC branches or filopodia. We define retraction or extension of ETC branches by an increase or decrease in the length above 2 μm within 60 min.

EXPECTED OUTCOMES

This protocol demonstrates a feasible method for Ca^{2+} and morphology imaging of ETCs in larval zebrafish. This method enables us to have an in-depth understanding on ETC behaviors via combining the spatiotemporal pattern of Ca^{2+} activities in ETCs (e.g., global/sub-cellular local Ca^{2+} activities and relative high-frequency/low-frequency/silent Ca^{2+} activities) (Figures 2 and 3B), and the growing state of ETCs (e.g., retraction/extension of ETC branches or filopodia, growing path selection of ETCs, or fusion between ETCs and targeting vessels) in intact larval zebrafish (Figure 4). Furthermore, using Ca^{2+} activities and morphological dynamics of ETCs as a readout, we are able to explore the involved regulation mechanism of ETC growth by intrinsic/extrinsic chemical or mechanical signals during vascular development.

For the source machinery of Ca^{2+} activities, both extracellular Ca^{2+} influx and intracellular Ca^{2+} store contributes to the generation of intracellular Ca^{2+} transients, and these two components can further interact to amplify the Ca^{2+} activity (Berridge et al., 2003). For example, the intracellular Ca^{2+} store opening mediated by inositol 1, 4, 5-trisphosphate receptors (IP3Rs) and ryanodine receptors (RyRs) are sensitive to the concentration of cytosolic Ca^{2+} , and they are identified to release Ca^{2+} from the endoplasmic reticulum/sarcoplasmic reticulum in a bell-shaped Ca^{2+} -response in response to the concentration of cytosolic Ca^{2+} (Bezprozvanny et al., 1991). Relative low concentration of cytosolic Ca^{2+} at nanomolar promotes the opening of IP3Rs and RyRs, leading to further increased content of cytosolic Ca^{2+} , which is the process known as Ca^{2+} -induced Ca^{2+} -store release. However, with the intracellular Ca^{2+} elevates, the relative high concentration of Ca^{2+} at micromolar instead inhibits the opening of IP3Rs and RyRs. On the other hand, the emptying Ca^{2+} store activates the extracellular Ca^{2+} influx through plasma membrane Ca^{2+} channels to replenish Ca^{2+} in the endoplasmic reticulum, a process known as store-operated Ca^{2+} entry (SOCE) (Oike et al., 1994; Vaca and Kunze, 1994). In endothelial cells, it has been reported that Ca^{2+} -store release and SOCE are required for the regulation of endothelial permeability or proliferation (Abdullaev et al., 2008; Oike et al., 1994; Sun et al., 2017; Vaca and Kunze, 1994), further some Ca^{2+} -store-related channels or transmembrane proteins located in the endoplasmic reticulum are identified for the regulation of EC migration during vascular morphogenesis (e.g., two-pore channels, TMEM33) (Favia et al., 2014; Savage et al., 2019). In parallel, previous study has shown that Ca^{2+} influx in ECs is required for EC proliferation or vessel invasion (Kohn et al., 1995), and our previous evidence also shows that Ca^{2+} activities in ETCs mediated by the mechanosensitive cationic channel Piezo1 plays a crucial role in vascular pathfinding (Liu et al., 2020). For the future study, it is intriguing to investigate the working mechanism and integration machinery of these Ca^{2+} components inside ETCs in response to various upstream inputs during vascular development.

LIMITATIONS

This protocol is applicable for Ca^{2+} imaging of ETCs with morphology mainly distributed in the X-Y plane due to the scan speed limitation. For ETCs with very long growing path and large sub-cellular branches/filopodia extending along the Z plane, the coverage of relatively increased number of frames spanned in the Z-axis may sacrifice the interval of time-lapse images to some extent for the current microscope parameters, thus optimized equipment setup for the confocal microscopy or the light-sheet imaging should be alternatively used.

The Ca^{2+} indicator GCaMP5 of the transgenic zebrafish *Tg(kdrl:GCaMP5)* line used in this protocol is expressed in ETCs, including the soma and branches. We did not find the expression of GCaMP5 in the filopodia of ETCs, neither Ca^{2+} activity inside. For monitoring Ca^{2+} activity in the filopodia of ETCs in larval zebrafish, other optimized transgenic lines for GCaMPs should be used. For this purpose, we tried the GCaMP6s indicator expressed in ECs of the transgenic *Tg(kdrl:GCaMP6s-CAAX)*

zebrafish larvae, and found that Ca^{2+} transients occurring in both filopodia and the mother branch of ETCs could be visualized when the Ca^{2+} transients are relative strong.

TROUBLESHOOTING

Problem 1

Poor fertilized egg production (production and maintenance of transgenic zebrafish larvae, step 2)

Potential solution

To get enough fertilized egg for the imaging experiment, the healthy state of adult male and female parental fish should be considered. Usually adult fish with the age younger than 2 years are used for egg production. Furthermore, to maintain a stable egg-producing ability of the adult fish, it is helpful to regularly mate the adult fish with the wild type fish (e.g., every 3 months). Alternatively, artificial insemination for adult fish could be used, while it may lead to disturbed healthy state for the adult fish.

Problem 2

For one batch of harvested zebrafish larvae used for imaging, some larvae display malformation or hemorrhage in the brain (production and maintenance of transgenic zebrafish larvae, steps 3–5).

Potential solution

Embryonic malformation or hemorrhage may happen with handling problems when transferring the larvae during maintaining. Always transfer the larvae gently using an appropriate clean and soft plastic straw with a smooth tip surface to avoid injury for the skin tissue of larvae. A new batch of larvae should be prepared if the percentage of malformation is relatively high.

Problem 3

Blood flow and heart beating of the imaged zebrafish larvae drop in the speed during the imaging process (imaging for Ca^{2+} activity and morphology of ETCs, step 5).

Potential solution

For long-term imaging on immobilized zebrafish larvae, the stress caused by accumulated metabolic waste and growing body-produced mechanical restriction may affect the healthy state of the larva and further the growing state of ETCs. To avoid this problem during imaging, it is helpful to keep an appropriate concentration of the lowing-melting point agarose (1.2%) when immobilizing the larvae, remove the agarose around the mouth and tail of the imaged larva to leave free space for growing, maintain an appropriate incubation temperature (28°C) for the larvae, and refresh the incubation medium every 30 min.

Problem 4

How to correct the motion artifacts at the X-Y plane in the image series (analysis of Ca^{2+} imaging data, step 6b)?

Potential solution

To correct motion artifacts at the X-Y plane within the same time-lapse image series, we align the image series with the selected reference image along X-Y plane using the Translation Transformation plugin in ImageJ (Figures 2B and 2C). The reference image selected within the image series should display obvious Ca^{2+} activity and relatively least movement at X-Y plane in the GCaMP5 series. For the selection of mCherry reference images, the image with the same sequential number with the GCaMP5 reference image should be used in the same time-lapse image series. For large motion artifact in the image series that cannot be corrected using the alignment procedure, we usually remove the largely moved images before analysis or remove data points of these images plotted in the $\Delta R/R_0$ dataset. On the other hand, our ratiometric analysis method using the fluorescence ratio of GCaMP5 to mCherry for $\Delta R/R_0$ calculation helps to reduce the effects of motion artifacts, as the

mCherry fluorescence also serves as a reference signal for GcaMP5 besides as a morphological indicator of ETCs.

Problem 5

Fluorophore bleaching of images occurred in the long-term confocal imaging experiment (imaging for Ca^{2+} activity and morphology of ETCs, step 5).

Potential solution

Based on our experience, the problem of fluorophore bleaching could be avoided through optimized laser scanning parameters. We usually capture images with spatial resolution of 0.2 – 0.4 μm per pixel, which is enough for achieving clear morphology of ETCs, including the branches and filopodia. When capturing images using the confocal microscope, on the basis of ensuring acceptable spatial resolution of the images, it is helpful to avoid the bleaching problem through appropriately (1) increasing the pinhole size and voltage of the photomultiplier tube (PMT); (2) decreasing the laser power/intensity, laser pixel dwell time, and scan magnification. In addition, it also helps to save the scan time for 3-dimensional time-lapse imaging through reducing the range of captured fields via the “crop” element in the imaging software combining with relative low scan magnification.

For Ca^{2+} imaging data contains obvious fluorophore bleaching, the declining tendency in Ca^{2+} trace ($\Delta F/F_0 - \text{Time (s)}$) could be corrected via applying adaptive F_0 values corresponding to each data point at each time point. In this protocol, our Ca^{2+} analysis script for excluding fluctuations in the baseline could overcome the problem in Ca^{2+} trace caused by fluorophore bleaching.

Problem 6

Artificial Ca^{2+} transients are included in the Ca^{2+} trace during analysis (analysis of Ca^{2+} imaging data, step 7).

Potential solution

For dataset containing sharp fluctuations in the baseline, the sharp fluctuations may be misclassified as Ca^{2+} transients by the script. To overcome this problem, dataset before and after the sharp fluctuation point of baseline should be separately analyzed. In addition, it is always recommended to perform Ca^{2+} activity analysis with this program using separated dataset cassettes according to the time length of the time-lapse dataset (e.g., for 10 – 30 min), as small cassette makes it more reliable to discriminate data points in the baseline or in the Ca^{2+} transients in the dataset, and easier to visually confirm the final-baseline removed Ca^{2+} trace and quantified Ca^{2+} transients. Finally, errors in identified Ca^{2+} transients because of large movements of images rather than Ca^{2+} activity of ETCs should be corrected manually.

RESOURCE AVAILABILITY

Lead contact

Further information and requests for resources and reagents should be directed to and will be fulfilled by the lead contact, Jiu-lin Du (forestdu@ion.ac.cn).

Materials availability

All unique/stable reagents generated in this study, including transgenic lines, mutants, and plasmids, are available from the Lead Contact without restriction.

Data and code availability

Code for data analysis generated is available in this study ([Data S2](#)).

SUPPLEMENTAL INFORMATION

Supplemental information can be found online at <https://doi.org/10.1016/j.xpro.2021.100388>.

ACKNOWLEDGMENTS

We thank Dr. Didier Stainier for providing the *Tg(kdrl:HRAS-mCherry)* line and Dr. Chunfeng Shang for suggestions on the kinetic analysis of Ca^{2+} transients. This work was supported by Shanghai Municipal Science and Technology Major Project (18JC1410100, 2018SHZDZX05), Key Research Program of Frontier Sciences (QYZDY-SSW-SMC028), Strategic Priority Research Program (XDB32010200) of Chinese Academy of Science, and Shanghai Leading Scientist Program. The graphical abstract was partially generated using the BioRender online software.

AUTHOR CONTRIBUTIONS

J.L.D. supervised the project. T.-t.L. and J.-I.D. designed experiments and wrote the manuscript. H.H. wrote the MATLAB code for analyzing Ca^{2+} transients.

DECLARATION OF INTERESTS

The authors declare no competing interests.

REFERENCES

- Abdullaev, I.F., Bisaillon, J.M., Potier, M., Gonzalez, J.C., Motiani, R.K., and Trebak, M. (2008). Stim1 and Orai1 mediate CRAC currents and store-operated calcium entry important for endothelial cell proliferation. *Circ. Res.* *103*, 1289–1299.
- Andrikopoulos, P., Fraser, S.P., Patterson, L., Ahmad, Z., Burcu, H., Ottaviani, D., Diss, J.K., Box, C., Eccles, S.A., and Djamgoz, M.B. (2011). Angiogenic functions of voltage-gated Na^+ channels in human endothelial cells: modulation of vascular endothelial growth factor (VEGF) signaling. *J. Biol. Chem.* *286*, 16846–16860.
- Berridge, M.J., Bootman, M.D., and Roderick, H.L. (2003). Calcium signalling: dynamics, homeostasis and remodelling. *Nat. Rev. Mol. Cell Biol.* *4*, 517–529.
- Bezprozvanny, I., Watras, J., and Ehrlich, B.E. (1991). Bell-shaped calcium-response curves of $\text{Ins}(1,4,5)\text{P}_3$ - and calcium-gated channels from endoplasmic reticulum of cerebellum. *Nature* *351*, 751–754.
- Carter, K.M., Woodley, C.M., and Brown, R.S. (2011). A review of tricaine methanesulfonate for anesthesia of fish. *Rev. Fish Biol. Fish.* *21*, 51–59.
- Chi, N.C., Shaw, R.M., De Val, S., Kang, G., Jan, L.Y., Black, B.L., and Stainier, D.Y. (2008). Foxn4 directly regulates *tbx2b* expression and atrioventricular canal formation. *Genes Dev.* *22*, 734–739.
- Favia, A., Desideri, M., Gambarà, G., D'Alessio, A., Ruas, M., Esposito, B., Del Bufalo, D., Parrington, J., Ziparo, E., et al. (2014). VEGF-induced neoangiogenesis is mediated by NAADP and two-pore channel-2-dependent Ca^{2+} signaling. *Proc. Natl. Acad. Sci. U S A* *111*, 4706–4715.
- Gordienko, D.V., and Tsukahara, H. (1994). Tetrodotoxin-blockable depolarization-activated Na^+ currents in a cultured endothelial cell line derived from rat interlobar arter and human umbilical vein. *Pflügers Arch.* *428*, 91–93.
- Kohn, E.C., Alessandro, R., Spoonster, J., Wersto, R.P., and Liotta, L.A. (1995). Angiogenesis: role of calcium-mediated signal transduction. *Proc. Natl. Acad. Sci. U S A* *92*, 1307–1311.
- Liu, T.T., Du, X.F., Zhang, B.B., Zi, H.X., Yan, Y., Yin, J.A., Hou, H., Gu, S.Y., Chen, Q., and Du, J.L. (2020). Piezo1-mediated Ca^{2+} activities regulate brain vascular pathfinding during development. *Neuron* *108*, 180–192.
- Oike, M., Gericke, M., Droogmans, G., and Nilius, B. (1994). Calcium entry activated by store depletion in human umbilical vein endothelial cells. *Cell Calcium* *16*, 367–376.
- Savage, A.M., Kurusamy, S., Chen, Y., Jiang, Z., Chhabria, K., MacDonald, R.B., Kim, H.R., Wilson, H.L., van Eeden, F.J.M., Armesilla, A.L., et al. (2019). *tmem33* is essential for VEGF-mediated endothelial calcium oscillations and angiogenesis. *Nat. Commun.* *10*, 732.
- Sun, M.Y., Geyer, M., and Komarova, Y.A. (2017). IP(3) receptor signaling and endothelial barrier function. *Cell. Mol. Life Sci.* *74*, 4189–4207.
- Yokota, Y., Nakajima, H., Wakayama, Y., Muto, A., Kawakami, K., Fukuhara, S., and Mochizuki, N. (2015). Endothelial Ca^{2+} oscillations reflect VEGFR signaling-regulated angiogenic capacity in vivo. *eLife* *4*, e08817.
- Vaca, L., and Kunze, D.L. (1994). Depletion of intracellular Ca^{2+} stores activates a Ca^{2+} -selective channel in vascular endothelium. *Am. J. Physiol.* *267*, 920–925.
- Westerfield, M. (2000). General methods for zebrafish care. In *The Zebrafish Book. A Guide for the Laboratory Use of Zebrafish (Danio rerio)*, Fourth Edition, M. Westerfield, ed. (University of Oregon Press).